



Revista Facultad de Ingeniería Universidad de Antioquia

ISSN: 0120-6230

revista.ingenieria@udea.edu.co

Universidad de Antioquia
Colombia

Rincón-Fulla, Marlon; Humberto-Marín, Jairo; Alberto-Suaza, Yoder
Two-electron energy levels in coupled nano-rings: the hydrostatic pressure and magnetic field effects
Revista Facultad de Ingeniería Universidad de Antioquia, núm. 73, diciembre, 2014, pp. 166-175
Universidad de Antioquia
Medellín, Colombia

Available in: <http://www.redalyc.org/articulo.oa?id=43032606015>

- How to cite
- Complete issue
- More information about this article
- Journal's homepage in redalyc.org

redalyc.org

Scientific Information System
Network of Scientific Journals from Latin America, the Caribbean, Spain and Portugal
Non-profit academic project, developed under the open access initiative

Two-electron energy levels in coupled nano-rings: the hydrostatic pressure and magnetic field effects

Niveles energéticos bi-electrónicos en nano-anillos acoplados: Efectos de la presión hidrostática y del campo magnético

Marlon Rincón-Fulla^{1,2}, Jairo Humberto-Marín^{2*}, Yoder Alberto-Suaza²

¹ Facultad de Ingeniería, Institución Universitaria Pascual Bravo. Cl 73 N.° 73A-226. AA. 6564. Medellín, Colombia.

² Escuela de Física, Universidad Nacional de Colombia. 59A N.° 63-20. AA. 3840, Medellín, Colombia.

(Received September 19, 2013; accepted May 19, 2014)

Abstract

The energy spectrum of two electrons spatially separated in two vertically coupled quantum rings under hydrostatic pressure and magnetic field is calculated. In order to study the two-electron properties, the adiabatic approximation is used by considering quantum rings with square cross-sections. The changes of the energy level-ordering and the crossover among the curves as a function of radii and ring-ring separation as well as the hydrostatic pressure and magnetic field are discussed. The effects related to the geometry of the rings as well as the external fields on the crystal Wigner formation are analyzed. Additionally, it is checked that the present results are in good agreement with those previously obtained for the limit cases corresponding to zero ring-ring separation and rings of equal center line radius.

-----**Keywords:** two electrons, vertically coupled quantum rings, energy spectrum, hydrostatic pressure

Resumen

Se calcula el espectro de energía dos electrones espacialmente separados en dos anillos cuánticos acoplados verticalmente bajo los efectos de presión hidrostática y de campo magnético. Para el estudio de las propiedades del sistema bi-electrónico se usa el método de aproximación adiabática considerando anillos cuánticos de sección transversal cuadrada. Se discuten

* Corresponding author: Jairo Humberto Marín, e-mail: mrfulla@pascualbravo.edu.co

los cambios en el ordenamiento de los niveles energéticos y el cruce entre las curvas como función de los factores geométricos más relevantes como son los radios y la separación entre anillos, así como la influencia de la presión hidrostática y del campo magnético. Se muestra el efecto de la geometría de los anillos así como el efecto de los campos sobre la formación de cristales de Wigner. Adicionalmente se comprueba que los resultados están en buen acuerdo con aquellos obtenidos para casos límites como son separación nula entre anillos y radios iguales.

-----**Palabras claves:** dos electrones, anillos acoplados verticalmente, espectro energético, presión hidrostática

Introduction

The rapid development in crystal growth technology have made possible to fabricate quantum dots (QDs) in different shapes [1, 2] such as, lenses, pyramids, disks and rings. The QDs profiles define different confinement potentials, which are used in the laboratory to research the accuracy of some approximated methods employed in the few-particle theory. Among the wide variety of QDs obtained experimentally, undoubtedly the quantum rings (QRs) have triggered the major interest because of the existence of an axially symmetric hole providing us different properties impossible to generate in other nanostructures. Particularly, the ground state electron confined into very narrow QRs as a function of the threading magnetic field strength undergoes the so-called Aharonov-Bohm oscillations (AB) [3, 4] whose period may be modified in QRs with non-homogenous cross-section [5-7] or by changing the QR center line radius [5-7].

Owing to the experimental creation of semiconductor quantum dots (QDs), a fascinating branch in physics has emerged linked to the electrons confined in low-dimensional systems. From the theoretical point of view, the interest on these systems is related with the purpose to understand the fundamental physics of few-particle systems in connection with the electronic interaction under the presence of external probes, such as hydrostatic pressure and electro-magnetic fields. The main reason for this interest is that the electron-electron interaction in semiconductor

nano-structures plays an important role in the optical and electrical transport properties at cryogenic temperatures.

The two-electron system is the simplest model that provides an excellent testing ground for various approximation methods, which are commonly used to analyze the correlation effects. This problem has been of interest almost since the advent of quantum mechanics and has been deeply studied for atoms and ions, such as H , He , Li^+ , etc., where the two electrons in these actual systems are kept by Coulomb confining potential. In recent years, the interest in this problem has arose again in connection with the study of the behavior of two electrons confined in quantum dots (QDs) where the Coulomb interaction is supplanted by a confinement potential. Different methods and models [8-13] have been used to investigate the energy spectrum and the electron-electron correlation effects in a quantum dots under the effect of an applied magnetic field. For instance, finite-differences [8], exact diagonalization within the effective-mass approximation [9], variational method [10], adiabatic approximation [11] and exact numerical methods [12-13] by considering two electrons into one [12] or two separated one-dimensional (1D) quantum rings (QRs) [13].

In the last few years, the fabrication of vertically stacked arrays of InAs self-assembled QDs have been reported [14]. These systems have shown to be more interesting than the isolated QDs because the ring-ring distance provides an additional degree of freedom to control the few-particle

energy spectrum which allows to explore new regimes of molecular physics [15] and improves the performance of optical devices through the quantum coupling between dots. In this context, we consider significant to explore the effects bound up with two electrons spatially separated in coupled QRs with vertical alignment under the hydrostatic pressure and magnetic field effects. In figure 1 we display a 3-dimensional picture for two vertically stacked QRs each one of them harboring an electron which is confined by a hard well confinement potential. In the present contribution, we propose a simple method based on the adiabatic approximation to calculate the two spatially separated electrons energy structure.

Brief Summary of model

In the effective-mass approximation, the two-electron Hamiltonian under the effects of hydrostatic pressure, P and z -direction magnetic field \vec{B} , can be written in cylindrical coordinates (ρ, ϕ, z) as shown in eq. (1a)

$$H = \sum_{j=1}^2 H_0(\vec{r}_j) + \frac{e^2}{\epsilon(P)|\vec{r}_2 - \vec{r}_1|} \quad (1a)$$

Where the one-electron Hamiltonian $H_0(\vec{r}_j)$ and electron-electron distance $|\vec{r}_2 - \vec{r}_1|$ are defined in eq. (1b) and eq. (1c), respectively

$$H_0(\vec{r}_j) = \frac{-\hbar^2}{2m^*(P)} \left[\frac{1}{\rho_j} \frac{\partial}{\partial \rho_j} \left(\rho_j \frac{\partial}{\partial \rho_j} \right) + \frac{1}{\rho_j^2} \frac{\partial^2}{\partial \phi_j^2} + \frac{\partial^2}{\partial z_j^2} \right] + \frac{i\hbar B}{2m^*(P)} \frac{\partial}{\partial \phi_j} + \frac{e^2 B^2 \rho_j^2}{8m^*(P)} + V_j(\rho_j, z_j) \quad (1b)$$

$$|\vec{r}_2 - \vec{r}_1| = \sqrt{\rho_1^2 + \rho_2^2 - 2\rho_1\rho_2\cos(\phi_2 - \phi_1) + (z_2 - z_1)^2} \quad (1c)$$

where \vec{r}_1 and \vec{r}_2 are the vector electron positions of electron 1 (e1) and electron 2 (e2), respectively (see Fig. 1). $V_j(\rho_j, z_j)$ is the j -electron confinement potential, equal to zero and infinite inside and outside the QR, respectively. The quantum ring geometrical parameters are defined through the width W and the center line radius R_1 (lower quantum ring) and R_2 (upper quantum ring). The coordinate's origin system has been located at the symmetry center of the lower QR.

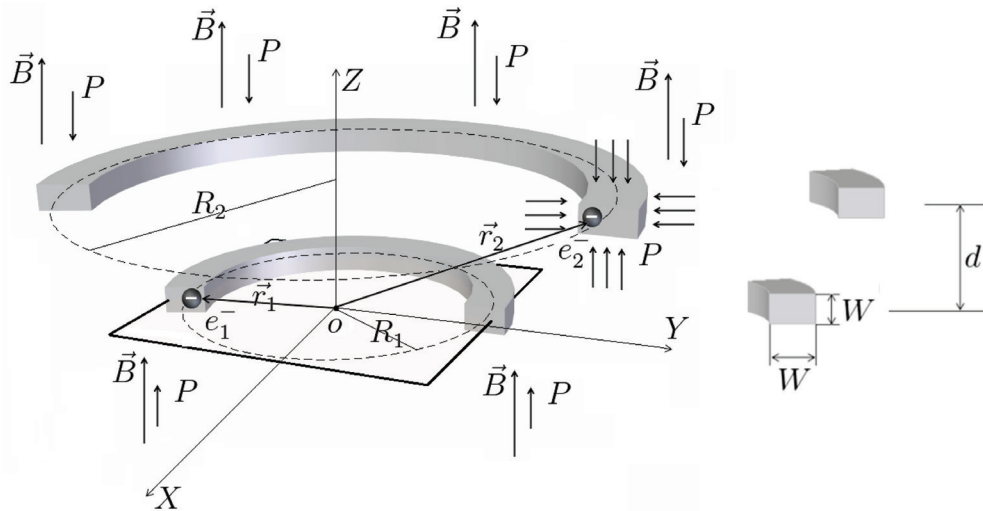


Figure 1 Pictorial view of two vertically coupled quantum rings considered in the present work. The geometry of the problem is also described being R_1 and R_2 the center line radii for lower and upper ring, respectively and d is the distance between rings

The effects of the hydrostatic pressure applied on the QRs have been included through the pressure dependence on the QR dimensions [16]: (height $W(P)$, inner and outer center line radii $R_{1,2}(P)$). These dependences are given through the eq. (2) and eq. (3):

$$W(P) = W(0)[1 - (S_{11} + 2S_{12})P]^{1/2} \quad (2)$$

$$R_j(P) = R_j(0) [1 - (S_{11} + 2S_{12})P]^{1/2} \quad (3)$$

Where $W(0)$ and R_j the QR height and center line QR radii without pressure applied, respectively. S_{11} and S_{12} are the GaAs compliance constants.

The hydrostatic pressure effects on the electron effective mass and dielectric permittivity are given by eq. (4) and eq. (5), respectively:

$$m^*(P) = m_0 \left[1 + \frac{\pi^2}{3} \left(\frac{2}{E_g^V(P)} + \frac{1}{E_g^V(P) + \Delta_0} \right) + \delta_m \right]^{-1} \quad (4)$$

$$\epsilon(P) = 12.74 \exp[-16.7 \cdot 10^{-4} P - 6.7 \cdot 10^{-3}] \quad (5)$$

where m_0 is the free electron mass and $E_g(P)$ is the pressure dependent GaAs band gap in meV, which is given by eq. (6):

$$E_g^V(P) = 1519.4 + 10.7P \quad (6)$$

In this work, kbar units are used in order to measure the hydrostatic pressure effects. The remaining parameters present in the above equations are according to reference [16].

By following the well-known results obtained by A. M. Elabasy [17] which demonstrated that the addition of the electron charge image term on the energy structure in semiconductor quantum wells increases the energy values in only one tenth of meV respect to the same model without considering the charge image term. Therefore and following others authors [18-21], we have considered in Hamiltonian (1) the bare electron-electron interaction. This repulsive Coulomb interaction in the Hamiltonian (1) makes impossible to find an exact solution, in consequence, an approximated method should

be implemented. On this subject, in Ref. [22] to analyze the A-B oscillations in concentric DQR has considered inner and outer center line radius equal to 83nm and 97nm, respectively. Besides, the experimental data about QRs have reported a height approximately equal to 2nm. With the above mentioned set of data, we can realize preliminary calculations based on the uncertainty relation to categorize the kinetic energy contributions in Hamiltonian (1). The kinetic energy (K) in radial (ρ) or axial (z) directions varies with $\sim 1/4R_i^2$ ($K_{\rho,z} \sim 1/16$) while the rotational energy around the z -axis varies with $\sim 1/R_{12}^2$ ($K_\phi \sim 1/(83)^2$) for inner ring or ($K_\phi \sim 1/(97)^2$) for outer ring. Therefore, the ratio between two energies $K_{\rho,z}/K_\phi$ for an electron into lower and upper quantum ring is approximately equal to 430 and 590, respectively. These results allow us to assure the applicability of the A.A in order to separate the slow rotation electron motion from the in plane rapid electron one. The A.A has yet to be shown to be a practical procedure for several nano-rings [23-25] because it is possible to reproduce the data for limit cases and from computational point of view is simpler than matrix diagonalization and variational methods. By following the model developed by Gutiérrez and co-workers [23] to reduce the D_2^+ 3-D Hamiltonian as well as the above mentioned facts and the substitution $\rho_j = R_j + \tilde{\rho}_j$ with normalized coordinates $\tilde{\rho}_j$ taking values between $-W/2$ and $W/2$, allows us to reduce the 3-D Schrodinger equation (1) to the following eigenvalue problem described by means of eq. (7a)

$$H = \sum_{j=1}^2 \left\{ \frac{-\hbar^2}{2m^*(P)} \left[\frac{1}{R_j^2} \frac{\partial^2}{\partial \varphi_j^2} + \frac{\partial^2}{\partial z_j^2} + \frac{ieB}{\hbar} \frac{\partial}{\partial \varphi_j} + \frac{e^2 B^2 \langle \rho_j^2 \rangle}{4\hbar^2 m^*(P)} \right] + V_j \right\} + \tilde{U}_{ee}(\varphi_2 - \varphi_1) + E_0 \quad (7a)$$

Where the meaning of the terms $\langle \rho_j^2 \rangle$ and $\tilde{U}_{ee}(\varphi_2 - \varphi_1)$ defined in eq. (7b) and eq. (7c), respectively, make reference to average values and they are discussed extensively in references [23-25].

$$\tilde{U}_{ee}(\varphi_2 - \varphi_1) = \frac{e^2}{\epsilon(P)} \left\langle f_0^{(1)} f_0^{(2)} \frac{1}{|\vec{r}_2 - \vec{r}_1|} \middle| f_0^{(1)} f_0^{(2)} \right\rangle \quad (7b)$$

$$\langle \rho_j^2 \rangle = \langle f_0^{(1)} f_0^{(2)} | \rho_j^2 | f_0^{(1)} f_0^{(2)} \rangle \quad (7c)$$

where $f_0^{(i)} = f_0^{(i)}(\rho, z_j)$ and E_0 are the exact wave function and the corresponding electron energy in a two-dimensional square quantum well with infinite barrier potential related to the electron motion along the cross-section. The eigenvalues E of the two-particle one-dimensional Schrodinger equation with Hamiltonian (7) can be solved by following the standard process, i.e., by using the center-of-mass $\Theta = (R_1^2 \varphi_1 + R_2^2 \varphi_2) / (R_1^2 + R_2^2)$ and relative coordinates $\varphi = \varphi_2 - \varphi_1$, which allows us to rewrite the Hamiltonian (7) as shown in eq. (8):

$$H = H_c + H_r \quad (8)$$

Being H_c and H_r the center-of-mass and relative terms, respectively. The exact eigen-values for center-of-mass term are given by eq. (9):

$$E_c(M) = \frac{\hbar^2}{2m^*(P)} \left[\frac{M^2}{R_1^2 + R_2^2} + MB + \frac{1}{4} B^2 \langle \rho_1^2 + \rho_2^2 \rangle \right] + E_0 \quad (9)$$

Where $M=0, \pm 1, \pm 2, \dots$ while the eigenvalues of the operator H_r denoted by $E_r(m, s)$ should be obtained numerically by solving the corresponding one-dimensional Schrodinger equation given by eq. (10):

$$H_r \psi_{m,s} = \left[-\frac{\hbar^2}{2m(P)} \left(\frac{1}{R_1^2} + \frac{1}{R_2^2} \right) \frac{d^2}{d\varphi^2} + \tilde{U}_{ee}(\varphi) \right] \psi_{m,s} = E_r(m, s) \psi_{m,s} \quad (10)$$

being $m=0, \pm 1, \pm 2, \dots$. The quantum numbers M and m define the center-of-mass and the two-electron relative angular momentum, respectively while $s = 0$ denotes even solutions or singlet states while and $s = 1$ denotes the odd solutions or triplet states.

Results and discussion

Before to display and carry out the discussion about the results obtained in the present work, it is pertinent to mention the way of denoting the two-electron total energy levels in QDs. In this work we use the same short notation a, b, c, \dots , etc whose corresponding quantum numbers (M, m, s) are listed in table 1.

Table 1 Energy levels of two electrons in quantum rings and renormalized energy for the limiting cases of Ref. [12]. The results were obtained at zero magnetic field and hydrostatic pressure. The energy unit employed in this table is the effective Rydberg $R_y^* = 5.93 \text{ meV}$ and effective Bohr radius $a_0^* = 100 \text{ \AA}$

Energy notation		$R=1a_0^*$		Energy notation		$R=4a_0^*$	
Short notation	Full Notation	Our Results	Ref. [12]	Short notation	Full notation	Our Results	Ref. [12]
a	$R^2 E(0,0,0)$	1.72	1.73	i	$R^2 E(1,3,1)$	11.90	11.90
b	$R^2 E(1,1,1)$	2.23	2.23	j	$R^2 E(3,1,0)$	12.41	12.41
c	$R^2 E(0,2,1)$	3.61	3.62	k	$R^2 E(2,2,0)$	13.40	13.40
d	$R^2 E(2,0,0)$	3.72	3.73	l	$R^2 E(0,4,1)$	15.71	15.71
e	$R^2 E(1,1,0)$	4.06	4.12	m	$R^2 E(4,0,0)$	13.18	13.18
f	$R^2 E(2,2,1)$	5.62	5.62	n	$R^2 E(1,3,0)$	16.19	16.21
g	$R^2 E(0,2,0)$	6.22	6.23	o	$R^2 E(3,3,1)$	15.90	15.90
h	$R^2 E(3,1,1)$	6.33	6.38	p	$R^2 E(4,2,1)$	15.92	15.92

We have checked the quality of the method employed in this work by comparing our results in the limit cases ($d \rightarrow 0$ and $W \rightarrow 0$) with those results reported in Ref. [12]. In order to compare the results, we have calculated the renormalized energy $\{R^2 E(M, m, s)\}$ with the same effective units than Ref. [12] (effective Bohr radius and effective Rydberg) for two different radii: $1a_0^* = 10 \text{ nm}$ (levels (a) to (h)) and $4a_0^* = 40 \text{ nm}$ (levels (i) to (p)). A rapid glance allows us to observe an

excellent agreement between both set of results for a single QR.

The total energy $E(M, m, s)$ as a function of the magnetic field strength is displayed in figure 2 for quantum rings with height $W = 20 \text{ \AA}$, zero ring-ring separation and zero hydrostatic pressure applied, for outer QR center line radius $R_2 = 400 \text{ \AA}$ with inner QR center line radius $R_1 = 375 \text{ \AA}$ and $R_1 = 300 \text{ \AA}$ are shown in upper panels from left to right.

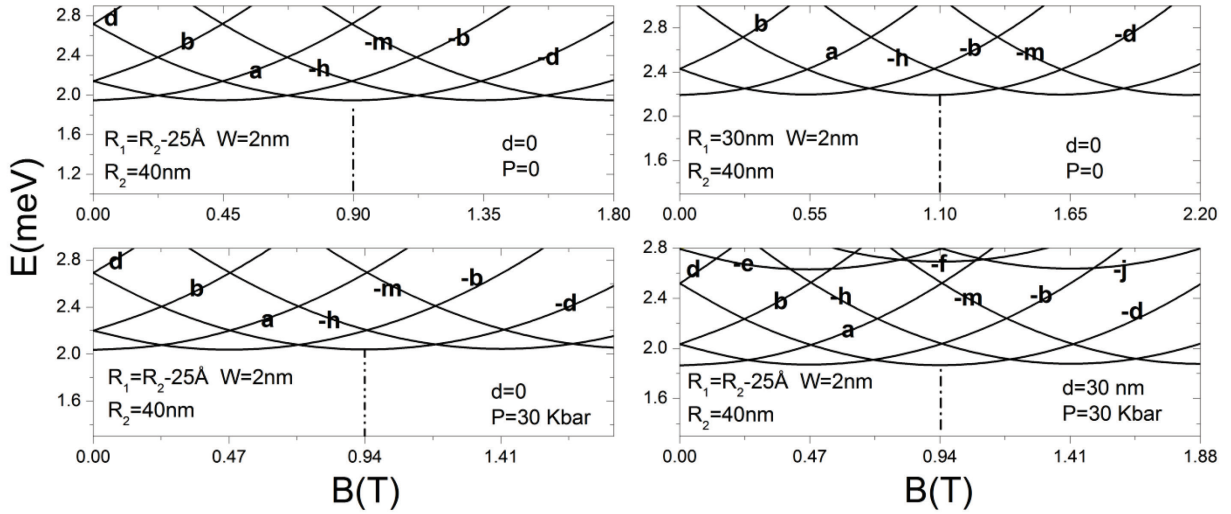


Figure 2 Low-lying energy levels for two electrons in vertically stacked quantum rings

The hydrostatic pressure on the low-lying energy levels versus magnetic field are shown in the lower panels for $P = 30 \text{ kbar}$ with ring-ring separation equal to zero (left lower panel) and 30 nm (check this number in Fig. 2) (right lower panel). All four graphics in figure 2 display B-periodic pattern called Aharonov-Bohm oscillations. This oscillatory behavior arises as a consequence of mixing the different angular momentum states of the center of mass M . An explanation for this remarkable effect can be given by comparing the contributions of paramagnetic term ($\sim B$) and diamagnetic one ($\sim B^2$). In consequence, for small magnetic field values, the paramagnetic term predominates over diamagnetic one, but this behavior is inverted for

large magnetic field values, which gives rise to a parabolic behavior of the energy having positive slope at the beginning when $M \geq 0$ or negatively slope when $M < 0$. This singular situation is only observed both experimentally and theoretically in ring-like systems due to the existence of a central crater which plays a decisive role in the purpose to fabricate novel opto-electronic devices.

In order to understand the hydrostatic pressure effect on the two-electron system in vertically coupled QRs it is necessary to take into account that non-zero applied pressure yields a reduction in the overall system in particular on the center line QR radii and the ring-ring separation. In consequence, the electron-electron distance tends

to diminish and the repulsive Coulomb interaction between them tends to increase. Therefore, the hydrostatic pressure effect for the center line radii considered in this figure is to rise up the ground state energy. For this reason is observed a slightly difference between the ground state energy levels at zero (left upper panel) and $P=30\text{kbar}$ (left lower panel). Another important difference between these curves is related to the A-B oscillations period which increases as measure as the hydrostatic pressure applied increases. This is because that period grows approximately as $1/(R_1^2(P)+R_2^2(P))$ and the difference between the center line radius at non zero and zero pressure applied is less than one, i.e., $[R_j(P \neq 0) - R_j(P=0)] < 1$. The geometrical effects on the two-electron structure may be inferred by collecting the left and right upper panels. In this regard, the upper panels for $d=0$ and $P=0$ corresponds to two concentric QRs, it is possible to observe that the greater are difference between QR center line radii the greater is the A-B oscillation period. This fact can be understood by calculating the electron-electron space pair correlation function [26] which allows us to demonstrate that the electron-electron average distance is greater in the configuration described in left upper panel than in the right upper panel. All these arguments are also valid to explain the difference between the right figures (upper and lower panels) where the change between both set of curves is due mainly to the major ring-ring separation since the hydrostatic pressure only modifies slightly the electron-electron energy structure. On these curves, the greater is the distance between the rings the smaller is the electron-electron repulsive Coulomb interaction which yields a diminishing in the electron-electron total energy.

From these two panels is observed the difference between the A-B oscillation periods. At the upper panel the A-B period is greater than in the lower one because the term $(R_1^2+R_2^2)$ is smaller.

Figure 3 shows the behavior of the ground state for two electrons in concentric QRs ($d=0$) with inner centerline radii $R_1=R_2-2.5\text{nm}$ as the outer center line radius varies from 20nm to 80nm

for three different values of the magnetic field strength 0, 0.67T, and 1.34T. The straight lines denote the evolution of the ground state energy at zero hydrostatic pressure applied while dashed lines are at 30kbar .

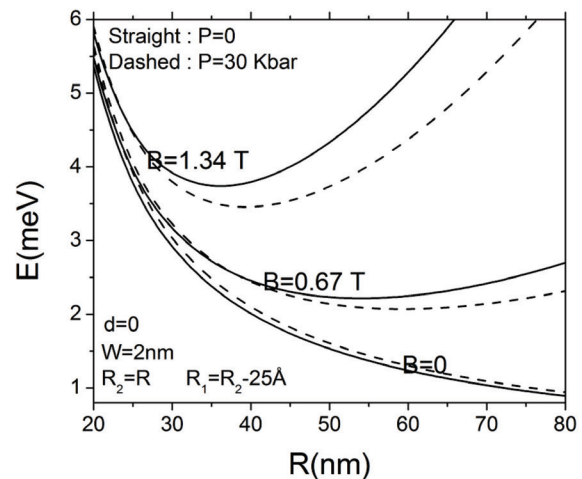


Figure 3 Two-electron ground state energy as a function of the outer center line quantum ring radius for different values of the magnetic field strength 0, 0.67T, 1.34T and two different values of hydrostatic pressure, zero (solid line) and 30kbar (dashed line)

From this figure is possible to observe for small radii of the center line that the electron-electron Coulomb interaction is really big since the mean distance between electrons is small which is responsible of the large values of two-electron energy. Nevertheless, for larger QR radii the repulsive term tends to disappear in consequence the system's spectrum gradually transforms to one corresponding to two independent rigid rotors since the electrons are not correlated. This behavior is observed for both zero and nonzero applied hydrostatic pressure. A remarkable result related to the crossovers between solid and dashed lines is observed at nonzero magnetic field strength. It is a consequence of the diamagnetic term in the center of mass energy ($\frac{1}{4} B^2 \langle \rho_1^2 + \rho_2^2 \rangle$) which tend to diminish as the hydrostatic pressure increase since the overall system shrinks its dimensions decreasing the total energy.

The effect of ring-ring separation on the total energy is shown in figure 4.

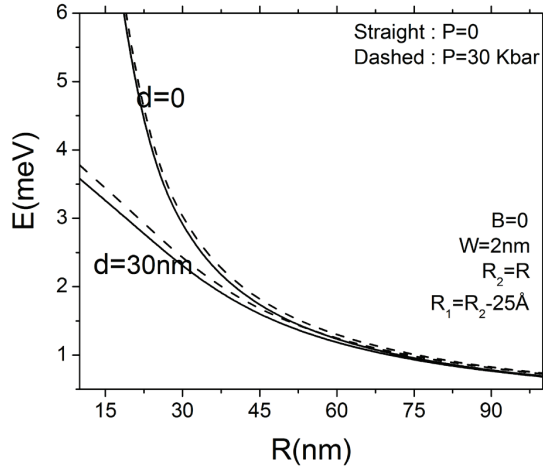


Figure 4 Two-electron ground state as a function of the outer center line quantum ring radius for two different values of the ring-ring separations 0, and 30nm for two different values of hydrostatic pressure zero (solid line) and 30kbar (dashed line)

For small outer center line radius, the smaller is the ring-ring separation the greater is the two-electron total energy both at zero and 30kbar of pressure applied. It is due to strong electron-electron correlation. Nevertheless, for outer center line radius greater than 75 nm the electron-electron repulsive term decrease substantially and the all curves asymptotically tend to merge into a single one which corresponds to two independent rigid rotors.

In figure 5, we display the evolution of the renormalized energy ($R^2 E$) as a function of the outer center line radius. In order to understand this figure is necessary to take in mind that the all curves are result of the strong competition between the renormalized kinetic energy ($R^2 \text{Kinetic Energy} \propto \frac{R^2}{R^2} = 1$) and renormalized potential energy ($R^2 \text{Potencial Energy} \propto \frac{R^2}{R} = R$). These dependences with the outer center line radius can be easily observed from Hamiltonian (1). In consequence, for large values of the outer quantum ring center line radius the renormalized potential energy predominates on the

renormalized kinetic energy and the curves tend to be quasi linear and the two-electron system tend as crystal like system while for small values of the center line radius, the renormalized kinetic energy predominates on the renormalized potential energy and the system is similar to gas with independent electrons. The dependences of the renormalized terms of the total energy with the center line radius is responsible for the intersections between different curves observed in figure 5. We have plotted the renormalized energy by following the same reasons described in references [12-13]. In this case the potential energy is proportional to outer center line radius R while the kinetic energy is approximately independent of this parameter.

We can see from the curves displayed in figure 5, for small values of the outer center line radius the slopes of the curves are changing. This fact shows the predominance of the renormalized kinetic energy on the renormalized repulsive Coulomb interaction. Nevertheless, this situation tends to invert as the outer center line radius tends to increases because the slopes of the curves tend to be constant which demonstrates the predominance of the renormalized potential energy. The constant value of the slope in the renormalized energy curves is an indicator of an ordered system where the repulsive Coulomb's energy predominates over the kinetic energy. This ordered configuration reached by the two-electron system is usually called as Wigner crystal.

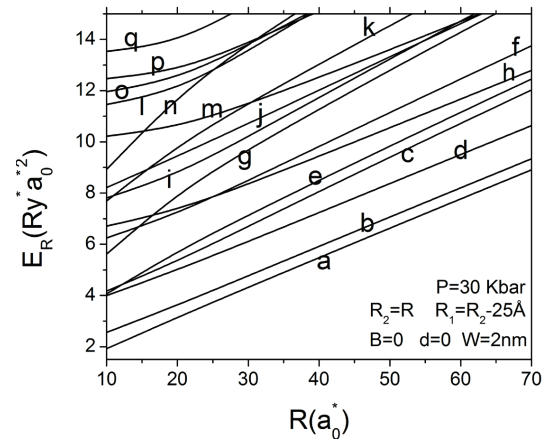


Figure 5 Renormalized total energy as a function of the outer center line radius for different states

Conclusions

We have studied some properties of the energy spectrum for electrons spatially separated and constrained to move in two vertically stacked toroidal quantum rings with square cross-section and different center line radii. We show that two-electron energy spectrum is strongly dependent on the external probes and geometrical parameters. In this regard, for small outer center line radius the predominance of the kinetic energy over the potential one allows us to obtain a disorder system similar to gas while the predominance of the potential energy over the kinetic one makes possible to obtain the ordered system similar to a crystal with only two electrons. These results are in good agreement with those previously reported for two electrons in one-dimensional rings.

Additionally, the external probes, magnetic field and hydrostatic pressure, tend to modify the two electron energy spectrum. In general, the application of hydrostatic pressure enhances the total energy due to the increasing of the electron-electron repulsion while the magnetic field yields a periodic oscillation of the two-electron ground state by increasing the magnetic field strength. This well-known effect is usually named as Aharonov–Bohm oscillations.

Acknowledgments

M. R. Fulla thanks to Institución Universitaria Pascual Bravo for the time in his working day to realize this research. J. H. Marín thanks to Facultad de Ciencias de la Universidad Nacional de Colombia- campus Medellín the economic aid to attend the OECS 2013

References

1. J. García, G. Medeiros, K. Schmidt, T. Ngo, J. Feng, A. Lorke, J. Kotthaus, P. Petroff, "Intermixing and shape changes during the formation of InAs self-assembled quantum dots". *Appl. Phys. Lett.* Vol. 71. 1997. pp. 2014-2016.
2. V. Fomin. *Physics of Quantum Rings*. 1st ed. Ed. Springer-Verlag. Berlin, Germany. 2014. pp. 1-264.
3. Y. Aharonov, D. Bohm. "Significance of Electromagnetic Potentials in the Quantum Theory". *Phys. Rev.* Vol. 115. 1959. pp. 485-491.
4. N. Kleemans, I. Bominaar, V. Fomin, V. Gladilin, D. Granados, A. Taboada, J. García, P. Offermans, U. Zeitler, P. Christianen, J. Maan, J. Devreese, P. Koenraad. "Oscillatory Persistent Currents in Self-Assembled Quantum Rings". *Phys. Rev. Lett.* Vol. 99. 2007. pp. 146808.
5. Y. Pershin, C. Piermarocchi. "Laser-controlled local magnetic field with semiconductor quantum rings". *Phys. Rev. B.* Vol. 72. 2005. pp. 245331.
6. A. Bruno, A. Latgé. "Aharonov-Bohm oscillations in a quantum ring: Eccentricity and electric-field effects". *Phys. Rev. B.* Vol. 71. 2005. pp. 125312.
7. J. Marín, W. Gutiérrez, I. Mikhailov. "An exciton trapped by an arbitrary shaped nanoring in a magnetic field". *J. Phys.: Conf. Ser.* Vol. 210. 2010. pp. 012045.
8. J. Planelles, J. Climente, F. Rajadell. "Quantum rings in tilted magnetic fields". *Physica E.* Vol. 33. 2006. pp. 370-375.
9. X. Wen. "A Two-Electron Quantum Ring Under Magnetic Fields". *Commun. Theor. Phys.* Vol. 49. 2008. pp. 1619-1621.
10. F. García, J. Marín, H. Paredes, I. Mikhailov. "Low-lying states of two-electron quasi-one-dimensional ring". *Phys. Status Solidi (c)*. Vol. 2. 2005. pp. 3630-3633.
11. F. Betancur, W. Gutiérrez, J. Piña. "Energy spectrum of on-axis negatively charged donor in toroidal-shaped ring". *Physica B.* Vol. 396. 2007. pp. 12-15.
12. J. Zhu, Z. Dai, X. Hu. "Two electrons in one-dimensional nanorings: Exact solutions and interaction energies". *Phys. Rev. B.* Vol. 68. 2003. pp. 045324.
13. J. Marín, F. García, I. Mikhailov. "Two electron in vertically coupled one-dimensional rings, Braz. Jour. Of Phys." Vol. 36. 2006. pp. 940-943.
14. S. Solomon, J. Trezza, A. Marshall, J. Harris. "Vertically Aligned and Electronically Coupled Growth Induced InAs Islands in GaAs". *Phys. Rev. Lett.* Vol. 76. 1996. pp. 952-955.
15. B. Partoens, F. Peeters. "Molecule-Type Phases and Hund's Rule in Vertically Coupled Quantum Dots". *Phys. Rev. Lett.* Vol. 84. 2000. pp. 4433-4436.
16. E. Reyes, N. Raigoza, L. Oliveira. "Effects of hydrostatic pressure and aluminum concentration on the conduction-electron g factor in GaAs-(Ga,Al)As

- quantum wells under in-plane magnetic fields". *Phys. Rev. B*. Vol. 77. 2008. pp. 115308.
17. A. Elabsy, "Effect of image forces on the binding energies impurity atoms in Ga1-xAlxAs-GaAs- Ga1-xAlxAs quantum wells". *Phys. Rev. B*. Vol. 46. 1992. pp. 2621-2624.
18. V. Fomin, V. Gladilin, S. Klimin, J. Devreese, N. Kleemans, P. Koenraad. "Theory of electron energy spectrum and Aharonov-Bohm effect in self-assembled InxGa1-xAs quantum rings in GaAs". *Phys. Rev. B*. Vol. 76. 2007. pp. 235320.
19. V. Fomin, V. Gladilin, J. Devreese, N. Kleemans, P. Koenraad. "Energy spectra and oscillatory magnetization of two-electron self-assembled InxGa1-xAs quantum rings in GaAs". *Phys. Rev. B*. Vol. 77. 2008. pp. 235326.
20. V. Fomin, V. Gladilin, J. Devreese, N. Kleemans, M. Bozkurt, P. Koenraad. "Electron and exciton energy spectra in self-assembled InGaAs/GaAs ring-like nanostructures". *Phys. Stat. Solidi (b)*. Vol. 245. 2008. pp. 2657-2661.
21. B. Monozon, P. Schmelcher. "Impurity center in a semiconductor quantum ring in the presence of crossed magnetic and electric fields". *Phys. Rev. B*. Vol. 67. 2008. pp. 045203.
22. G. Chen, Y. Chen, D. Chuu. "The Aharonov-Bohm effect in concentric quantum double rings". *Solid State Communications*. Vol. 143. 2007. pp. 515-518.
23. W. Gutiérrez, L. García, I. Mikhailov. "Coupled donors in quantum ring in a threading magnetic field". *Physica E*. Vol. 43. 2010. pp. 559-566.
24. J. Marín, M. Fulla, F. Rodríguez, F. García, J. Piña. "Spectral properties of two electrons vertically coupled in toroidal quantum rings". *Superlatt. Microstruct.* Vol. 49. 2011. pp. 252-257.
25. M. Fulla, J. Marín, W. Gutiérrez, M. Mora, C. Duque. "Essential properties of a D2+ molecular complex confined in ring-like nanostructures under external probes: Magnetic field and hydrostatic pressure". *Superlatt. Microstruct.* Vol. 67. 2011. 207-220.
26. I. Mikhailov, L. García, J. Marín. "Effect of wetting layer on electron-hole correlation in quantum discs and rings". *J. Phys.: Condens. Matter*. Vol. 18. 2006. pp. 9493-9507.